A carbon–oxygen-bridged hexacyclic ladder-type building block for low-bandgap nonfullerene acceptors†

Ting Li,‡[ab] Honghong Zhang,‡[b] Zuo Xiao, [b] Jeromy J. Rech, [c] Helin Niu,*[a] Wei You *[c] and Liming Ding *[b]

A hexacyclic carbon–oxygen-bridged ladder-type unit, CO$_i$6, was developed. Three nonfullerene acceptors (CO$_i$6IC, CO$_i$6FIC and CO$_i$6DFIC) based on CO$_i$6 were prepared. They present low optical bandgaps of 1.31–1.37 eV and strong absorbance in the near-infrared region. A 9.12% power conversion efficiency was achieved from the solar cells based on CO$_i$6FIC and a wide-bandgap copolymer donor (FTAZ).

Recently, acceptor–donor–acceptor (A–D–A) small molecules have emerged as efficient acceptor materials for organic solar cells (OSCs).[1] These molecules generally consist of a ladder-type electron-donating core unit and two strong electron-withdrawing end units.[2] The merits of A–D–A acceptors are as follows: (1) tunable energy levels and good electron mobility to match donor materials; (2) strong visible and near-infrared (NIR) absorption to generate more excitons; (3) out-of-plane side chains to avoid over aggregation and to realize optimal morphology.[3] Over 14% power conversion efficiency (PCE) was first reported by Ding *et al.*[4]

Molecular engineering *via* tailoring the structures of core units, end units and the side chains is the key toward high-performance A–D–A nonfullerene acceptors.[5] Recently, our group has developed novel carbon–oxygen-bridged (CO-bridged) ladder-type core units for making efficient A–D–A acceptors.[6] Compared with carbon-bridged (C-bridged) units, CO-bridged units show enhanced electron-donating capability and planarity. CO-Bridged A–D–A acceptors present narrower bandgaps, stronger light-harvesting capability, higher electron mobility and better photovoltaic performance.[6] Low-bandgap nonfullerene materials have attracted great attention due to their potential application in semi-transparent solar cells,[7] tandem solar cells,[8] and photodetectors.[9] Therefore, developing new low-bandgap CO-bridged A–D–A acceptors is quite necessary. Here, we report the preparation of a hexacyclic CO-bridged ladder-type building block, CO$_i$6, and the use of CO$_i$6 in making three low-bandgap A–D–A acceptors, CO$_i$6IC, CO$_i$6FIC and CO$_i$6DFIC (Fig. 1). The optical, electrochemical properties and the photovoltaic performance of CO$_i$6-based acceptors were investigated. Fluorine-substitution in the end units significantly affects the performance of the acceptors. Solar cells based on CO$_i$6FIC and a wide-bandgap copolymer donor, poly(4-(5-(4,8-bis(3-butylnonyl)benzo[1,2-*b*:4,5-*b'*]dithiophen-2-yl)thiophen-2-yl)-2-(2-butyloctyl)-5,6-difluoro-7-(thiophen-2-yl)-2*H*-benzo[*d*][1,2,3]triazole) (FTAZ),[10] gave a PCE of 9.12%.

The synthetic route is shown in Scheme 1. Stille coupling of (3,6-dimethoxythieno[3,2-*b*]thiophene-2,5-diyl)bis(trimethyl-stannane) and 2-ethylhexyl 2-bromothiophene-3-carboxylate gave compound **1** in 83% yield. Treating compound **1** with BBr$_3$ afforded the demethylated compound **2** in 95% yield. Compound **2** was quantitatively converted to bislactone **3** *via* an acid-promoted intramolecular transesterification.[6b] The addition of four equivalents of Grignard reagent to **3** followed by an intramolecular dehydration cyclization afforded CO$_i$6 in 86% yield.[11] "i" indicates that C–O bonds point to the core of the molecule (inward), and "6" stands for six fused rings. Deprotonation of CO$_i$6 by BuLi followed by adding *N*,*N*-dimethylformamide (DMF) produced CO$_i$6–CHO in 80% yield. Finally, Knoevenagel condensation of CO$_i$6–CHO with 1,1-dicyanomethylene-3-indanone (IC), monofluoro-substituted IC (FIC) or difluoro-substituted IC (DFIC) afforded CO$_i$6IC, CO$_i$6FIC and CO$_i$6DFIC in 90%, 94% and 86% yields, respectively. The structures of the compounds were confirmed by nuclear magnetic resonance (NMR) and mass spectroscopy (see ESI†). These compounds show good solubility in common solvents such as chloroform, toluene and chlorobenzene.

[a] *School of Chemistry & Chemical Engineering, Anhui Province Key Laboratory of Chemistry for Inorganic/Organic Hybrid Functionalized Materials, Anhui University, Hefei 230601, China. E-mail: niuhelin@ahu.edu.cn*

[b] *Center for Excellence in Nanoscience (CAS), Key Laboratory of Nanosystem and Hierarchical Fabrication (CAS), National Center for Nanoscience and Technology, Beijing 100190, China. E-mail: ding@nanoctr.cn*

[c] *Department of Chemistry, University of North Carolina at Chapel Hill, NC 27599, USA. E-mail: wyou@unc.edu*
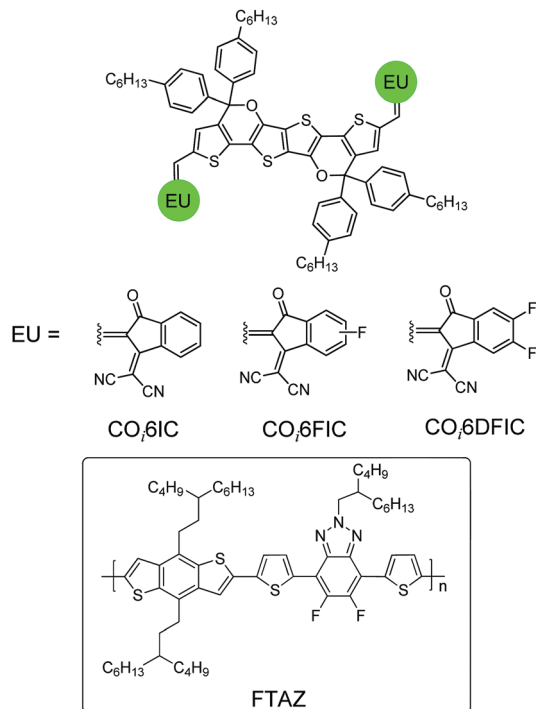
Fig. 1 The structures of COᵢ6IC, COᵢ6FIC, COᵢ6DFIC and FTAZ.

Fig. 2 Absorption spectra for COᵢ6IC, COᵢ6FIC, COᵢ6DFIC and FTAZ films.

Scheme 1 The synthetic routes for COᵢ6IC, COᵢ6FIC and COᵢ6DFIC.

The absorption spectra for CO₆IC, CO₆FIC, CO₆DFIC and FTAZ in chloroform and as films are shown in Fig. S15 (ESI†) and Fig. 2, respectively. In solution, CO₆IC, CO₆FIC and
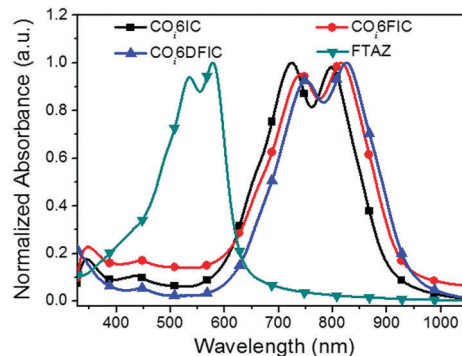
CO₆DFIC show a strong intramolecular charge transfer (ICT) band at 600–850 nm, with a low-energy peak at 755 nm, 764 nm and 769 nm, respectively, and a shoulder absorption at 697 nm, 701 nm and 702 nm, respectively (Table 1). For films, the absorption show bathochromic shifts and the shoulder absorption intensifies. From solution to film, the redshifts for the low-energy peaks of CO₆IC, CO₆FIC and CO₆DFIC are 40 nm, 51 nm and 55 nm, respectively, suggesting that the fluorination on IC unit enhanced the intermolecular interaction. The optical bandgaps (E_g^{opt}) estimated from the absorption onsets of CO₆IC, CO₆FIC and CO₆DFIC films are 1.37 eV, 1.34 eV and 1.31 eV, respectively. Small E_g^{opt} suggests strong electron-donating capability of CO₆ unit.[12] Fluorine atoms enhance electron-withdrawing capability of the end units and strengthen the ICT, leading to a bandgap shrink. FTAZ film absorbs 350–650 nm light, which is complementary to CO₆ acceptors (600–950 nm). The energy levels estimated from CV measurements are shown in Fig. 3.[13] The highest occupied molecular orbital (HOMO) levels for CO₆IC, CO₆FIC and CO₆DFIC are −5.57 eV, −5.60 eV and −5.64 eV, respectively, and the lowest unoccupied molecular orbital (LUMO) levels are −3.86 eV, −3.93 eV and −4.04 eV, respectively. Fluorine atoms lower both HOMO and LUMO levels, but they lower LUMO more. The donor FTAZ exhibits a HOMO at −5.36 eV and a LUMO at −3.05 eV.

Bulk heterojunction solar cells with a structure of ITO/ZnO/FTAZ:acceptor/MoO₃/Ag were fabricated to evaluate the performance of CO₆ acceptors.[14] The optimized conditions for FTAZ:CO₆IC, FTAZ:CO₆FIC and FTAZ:CO₆DFIC solar cells are the same: a D/A ratio of 1:1.6 (w/w), an active layer thickness of ∼85 nm and 0.2 vol% 1,8-diiodooctane (DIO) as the additive (Tables S1–S9, ESI†). J–V curves and external quantum efficiency (EQE) spectra for the best cells are shown in Fig. 4, and the performance data are listed in Table 2. Fluorine substitution can significantly affect the performance of CO₆ acceptors. The open-circuit voltages (V_{oc}) for CO₆IC, CO₆FIC and CO₆DFIC cells are 0.82 V, 0.75 V and 0.67 V, respectively. V_{oc} decreasing along with fluorine substitution is due to LUMO descending, since V_{oc} is proportional to (LUMO$_{acceptor}$−HOMO$_{donor}$).[15] In contrast, the short-circuit current densities (J_{sc}) increase along with fluorine substitution. J_{sc} of 17.45 mA cm⁻², 19.38 mA cm⁻² and 20.98 mA cm⁻² were obtained from CO₆IC, CO₆FIC and CO₆DFIC cells, respectively. With fluorine substitution,

Table 1 Optical and electrochemical data for the acceptors

Acceptors	λ_{sol} [nm]	λ_{film} [nm]	λ_{on} [nm]	$E_g^{opt\,a}$ [eV]	E_{ox}^{on} [V]	E_{red}^{on} [V]	HOMO[b] [eV]	LUMO[c] [eV]	$E_g^{ec\,d}$ [eV]
CO$_i$6IC	697, 755	722, 795	903	1.37	0.77	−0.94	−5.57	−3.86	1.71
CO$_i$6FIC	701, 764	739, 815	927	1.34	0.80	−0.87	−5.60	−3.93	1.67
CO$_i$6DFIC	702, 769	749, 824	945	1.31	0.84	−0.76	−5.64	−4.04	1.60

[a] $E_g^{opt} = 1240/\lambda_{on}$. [b] HOMO $= -(E_{ox}^{on} + 4.8)$. [c] LUMO $= -(E_{red}^{on} + 4.8)$. [d] $E_g^{ec} = $ LUMO $-$ HOMO.

Fig. 3 Energy level diagram.

Table 2 Performance data for the solar cells

D:A	V_{oc} [V]	J_{sc} [mA cm^{-2}]	FF [%]	PCE [%]
FTAZ:CO$_i$6IC	0.82	17.45 (16.93)[a]	59.0	8.43 (8.35)[b]
FTAZ:CO$_i$6FIC	0.75	19.38 (19.27)	62.6	9.12 (9.02)
FTAZ:CO$_i$6DFIC	0.67	20.98 (20.39)	58.9	8.25 (8.11)

[a] The data in the parentheses are integrated current density from EQE spectra. [b] The data in the parentheses are averages for 10 cells.

To understand the fluorination effect on the photovoltaic performance of CO$_i$6 acceptors, we first studied the exciton dissociation probabilities (P_{diss}) in different cells (Fig. 5a).[16] P_{diss} for CO$_i$6IC, CO$_i$6FIC and CO$_i$6DFIC cells are 90.4%, 94.1% and 93.9%, respectively. Higher P_{diss} for CO$_i$6FIC and CO$_i$6DFIC cells indicate that fluorination favors the generation of free charge carriers. This explains the higher EQE and J_{sc} of CO$_i$6FIC and CO$_i$6DFIC cells than that of CO$_i$6IC cells. We studied bimolecular recombination by plotting J_{sc} against light intensity (P_{light}) (Fig. 5b).[17] The data were fitted to a power law: $J_{sc} \propto P_{light}^{\alpha}$. The α values for CO$_i$6IC, CO$_i$6FIC and CO$_i$6DFIC cells are 0.978, 0.987 and 0.983,

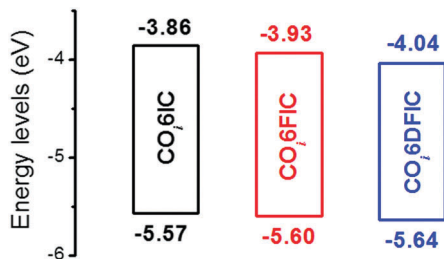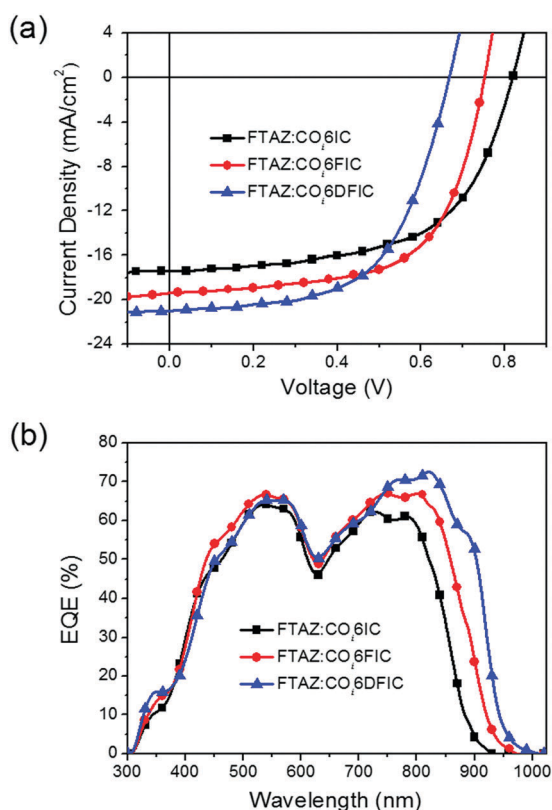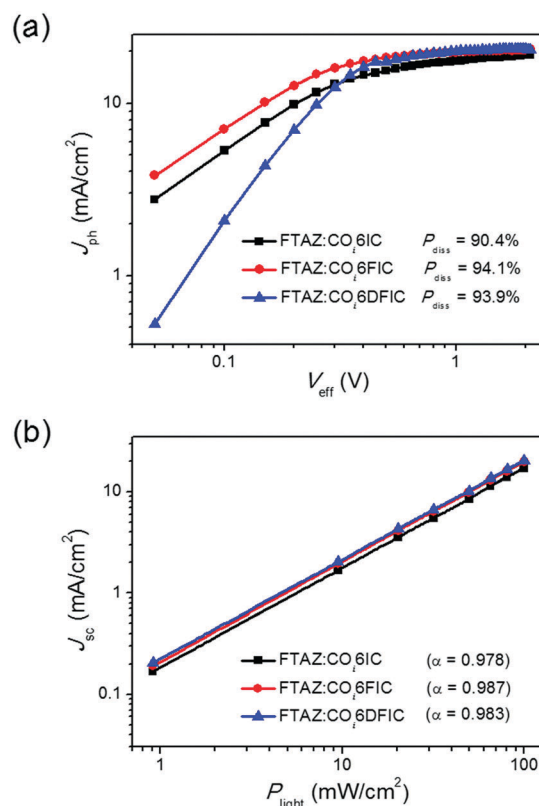**Fig. 4** J–V curves (a) and EQE spectra (b) for the solar cells.

the EQE spectra broaden and intensify (Fig. 4b). The broadening of EQE spectra results from the enhanced light-harvesting capability of the acceptors, while enhanced EQE might result from the improved charge generation and transport in the active layer. The integrated photocurrent densities from EQE spectra are consistent with J_{sc} from J–V measurements (Table 2). The fill factors (FF) for CO$_i$6IC, CO$_i$6FIC and CO$_i$6DFIC cells are 59.0%, 62.6% and 58.9%, respectively. CO$_i$6FIC solar cells gave the highest PCE of 9.12%.

Fig. 5 (a) J_{ph}–V_{eff} plots; (b) J_{sc}–P_{light} plots.

respectively, suggesting that solar cells using fluorinated acceptors have less charge recombination. Charge carrier mobilities were evaluated by using space charge limited current (SCLC) method (Fig. S17 and S18, ESI†).[18] Compared with FTAZ:CO$_i$6IC blend film, the hole and electron mobilities (μ_h and μ_e) simultaneously got improved in FTAZ:CO$_i$6FIC and FTAZ:CO$_i$6DFIC blend films (Table S10, ESI†). FTAZ:CO$_i$6FIC film shows the highest μ_h and μ_e of 1.45×10^{-4} cm^2 V^{-1} s^{-1} and 2.07×10^{-5} cm^2 V^{-1} s^{-1}, respectively. FTAZ:CO$_i$6FIC film presents the most balanced charge carrier transport, thus delivering the highest FF.

Film morphology was studied by using atomic force microscope (AFM) (Fig. S19, ESI†). FTAZ:CO$_i$6FIC blend film gives the smoothest surface among the three films. The root-mean-square roughnesses for FTAZ:CO$_i$6IC, FTAZ:CO$_i$6FIC and FTAZ:CO$_i$6DFIC films are 2.33 nm, 0.94 nm and 1.87 nm, respectively. FTAZ:CO$_i$6FIC blend film presents the finest nanofibers with diameters around 12 nm. With appropriate fluorination at the end units of the acceptor, the donor and acceptor materials can present a suitable miscibility and can make ideal nanoscale phase separation for efficient charge generation and transport, thus delivering optimal photovoltaic performance.

Conclusions

In summary, a CO-bridged hexacyclic core unit (CO$_i$6) and three A–D–A nonfullerene acceptors were developed. Owing to the strong electron-donating capability of CO$_i$6, these acceptors present narrow optical bandgaps and good NIR absorption. The energy levels, light absorption, mobilities, and the miscibility between donor and acceptor materials can be tuned *via* fluorination. Solar cells based on a wide-bandgap polymer donor (FTAZ) and CO$_i$6 acceptors gave decent PCEs, and FTAZ:CO$_i$6FIC cells delivered the highest PCE of 9.12%. This work also demonstrates the great potential of CO-bridged low-bandgap nonfullerene acceptors.

Conflicts of interest

There are no conflicts to declare.

Acknowledgements

References

1 (*a*) Y. Lin and X. Zhan, *Mater. Horiz.*, 2014, **1**, 470; (*b*) W. Chen and Q. Zhang, *J. Mater. Chem. C*, 2017, **5**, 1275; (*c*) S. Li, Z. Zhang, M. Shi, C.-Z. Li and H. Chen, *Phys. Chem. Chem. Phys.*, 2017, **19**, 3440.

2 Y. Lin, J. Wang, Z. G. Zhang, H. Bai, Y. Li, D. Zhu and X. Zhan, *Adv. Mater.*, 2015, **27**, 1170.

3 Y. Lin, F. Zhao, Y. Wu, K. Chen, Y. Xia, G. Li, S. K. K. Prasad, J. Zhu, L. Huo, H. Bin, Z. G. Zhang, X. Guo, M. Zhang, Y. Sun, F. Gao, Z. Wei, W. Ma, C. Wang, J. Hodgkiss, Z. Bo, O. Inganäs, Y. Li and X. Zhan, *Adv. Mater.*, 2017, **29**, 1604155.

4 Z. Xiao, X. Jia and L. Ding, *Sci. Bull.*, 2017, **62**, 1562.

5 (*a*) J. Wang, W. Wang, X. Wang, Y. Wu, Q. Zhang, C. Yan, W. Ma, W. You and X. Zhan, *Adv. Mater.*, 2017, **29**, 1702125; (*b*) S. Dai, F. Zhao, Q. Zhang, T.-K. Lau, T. Li, K. Liu, Q. Ling, C. Wang, X. Lu, W. You and X. Zhan, *J. Am. Chem. Soc.*, 2017, **139**, 1336; (*c*) Y. Lin, F. Zhao, Q. He, L. Huo, Y. Wu, T. C. Parker, W. Ma, Y. Sun, C. Wang, D. Zhu, A. J. Heeger, S. R. Marder and X. Zhan, *J. Am. Chem. Soc.*, 2016, **138**, 4955.

6 (*a*) Z. Xiao, F. Liu, X. Geng, J. Zhang, S. Wang, Y. Xie, Z. Li, H. Yang, Y. Yuan and L. Ding, *Sci. Bull.*, 2017, **62**, 1331; (*b*) Z. Xiao, X. Jia, D. Li, S. Wang, X. Geng, F. Liu, J. Chen, S. Yang, T. P. Russell and L. Ding, *Sci. Bull.*, 2017, **62**, 1494.

7 (*a*) W. Wang, C. Yan, T.-K. Lau, J. Wang, K. Liu, Y. Fan, X. Lu and X. Zhan, *Adv. Mater.*, 2017, **29**, 1701308; (*b*) F. Liu, Z. Zhou, C. Zhang, J. Zhang, Q. Hu, T. Vergote, F. Liu, T. P. Russell and X. Zhu, *Adv. Mater.*, 2017, **29**, 1606574.

8 W. Liu, S. Li, J. Huang, S. Yang, J. Chen, L. Zuo, M. Shi, X. Zhan, C.-Z. Li and H. Chen, *Adv. Mater.*, 2016, **28**, 9729.

9 W. Wang, F. Zhang, H. Bai, L. Li, M. Gao, M. Zhang and X. Zhan, *Nanoscale*, 2016, **8**, 5578.

10 S. C. Price, A. C. Stuart, L. Yang, H. Zhou and W. You, *J. Am. Chem. Soc.*, 2011, **133**, 4625.

11 L. Dou, C.-C. Chen, K. Yoshimura, K. Ohya, W.-H. Chang, J. Gao, Y. Liu, E. Richard and Y. Yang, *Macromolecules*, 2013, **46**, 3384.

12 H. Zhou, L. Yang and W. You, *Macromolecules*, 2012, **45**, 607.

13 Z. Xiao, G. Ye, Y. Liu, S. Chen, Q. Peng, Q. Zuo and L. Ding, *Angew. Chem., Int. Ed.*, 2012, **51**, 9038.

14 Z. Xiao, X. Geng, D. He, X. Jia and L. Ding, *Energy Environ. Sci.*, 2016, **9**, 2114.

15 B. P. Rand, D. P. Burk and S. R. Forrest, *Phys. Rev. B: Condens. Matter Mater. Phys.*, 2007, **75**, 115327.

16 J.-L. Wu, F.-C. Chen, Y.-S. Hsiao, F.-C. Chien, P. Chen, C.-H. Kuo, M. H. Huang and C.-S. Hsu, *ACS Nano*, 2011, **5**, 959.

17 M. An, F. Xie, X. Geng, J. Zhang, J. Jiang, Z. Lei, D. He, Z. Xiao and L. Ding, *Adv. Energy Mater.*, 2017, **7**, 1602509.

18 J. Cao, Q. Liao, X. Du, J. Chen, Z. Xiao, Q. Zuo and L. Ding, *Energy Environ. Sci.*, 2013, **6**, 3224.